

RESEARCH

Open Access



Application of a novel biological-nanoparticle pretreatment to *Oscillatoria acuminata* biomass and coculture dark fermentation for improving hydrogen production

Mostafa El-Sheekh^{1†}, Mostafa Elshobary^{1*†}, Eman Abdullah¹, Refat Abdel-Basset² and Metwally Metwally¹

Abstract

Background Energy is the basis and assurance for a world's stable development; however, as traditional non-renewable energy sources deplete, the development and study of renewable clean energy have emerged. Using microalgae as a carbon source for anaerobic bacteria to generate biohydrogen is a clean energy generation system that both local and global peers see as promising.

Results *Klebsiella pneumonia*, *Enterobacter cloacae*, and their coculture were used to synthesize biohydrogen using *Oscillatoria acuminata* biomass via dark fermentation. The total carbohydrate content in *O. acuminata* was 237.39 mg/L. To enhance the content of fermentable reducing sugars, thermochemical, biological, and biological with magnesium zinc ferrite nanoparticles (Mg-Zn Fe₂O₄-NPs) pretreatments were applied. Crude hydrolytic enzymes extracted from *Trichoderma harzianum* of biological pretreatment were enhanced by Mg-Zn Fe₂O₄-NPs and significantly increased reducing sugars (230.48 mg/g) four times than thermochemical pretreatment (45.34 mg/g). *K. pneumonia* demonstrated a greater accumulated hydrogen level (1022 mLH₂/L) than *E. cloacae* (813 mLH₂/L), while their coculture showed superior results (1520 mLH₂/L) and shortened the production time to 48 h instead of 72 h in single culture pretreatments. Biological pretreatment + Mg-Zn Fe₂O₄ NPs using coculture significantly stimulated hydrogen yield (3254 mLH₂/L), hydrogen efficiency)216.9 mL H₂/g reducing sugar(and hydrogen production rate (67.7 mL/L/h) to the maximum among all pretreatments.

Conclusion These results confirm the effectiveness of biological treatments + Mg-Zn Fe₂O₄-NPs and coculture dark fermentation in upregulating biohydrogen production.

Keywords Biohydrogen, Biological pretreatment, Thermochemical, Coculture, Dark fermentation, Nanoparticles

[†]Mostafa El-Sheekh and Mostafa Elshobary are co-first authors

*Correspondence:

Mostafa Elshobary

mostafa_elshobary@science.tanta.edu.eg

¹ Department of Botany, Faculty of Science, Tanta University, Tanta 31527, Egypt

² Botany and Microbiology Department, Faculty of Science, Assuit University, Assuit, Egypt

Background

Recent years have seen a rise in the use of sustainable and clean fuels, particularly biofuels, due to the high expense of fossil fuels and their detrimental impact on the environment [1, 2]. Scientists are becoming more interested in biofuels because they are environmentally friendly and made from affordable, non-edible, and inexpensive



feedstocks [3–5]. Hydrogen is typically deemed as a cleaner and more promising contender due to the most incredible energy output of any other fuel (143 GJ tonne⁻¹). In addition, it is the only known fuel that doesn't emit CO₂ as a byproduct in combusting engine. Biological hydrogen synthesis from algae is interpreted as one of the most talented green power generation solutions [6]. Hydrogen synthesis from algae is investigated as an alternative form of energy for power generation with the development and commercialization of fuel cells. Presently, sugarcane and maize as starch-rich crops and lignocellulosic raw materials (such as rice straw and agriculture wastes) are utilized as biomass feedstocks for biofuel.

Nevertheless, exploiting agricultural crops or wastes for biofuel production presents challenges owing to limited arable land and water supplies [7]. Furthermore, the increased cost of digestion of lignocellulosic biomass is one of the technique's weaknesses owing to the high lignin concentration in biomass, making the saccharification process challenging [8, 9]. Lately, microalgae, including cyanobacteria, have been proposed as a third-generation feedstock for biofuel production [6, 8]. Furthermore, microalgae species accumulate significant content of carbohydrates in the form of starch, glycogen, and cellulose, that consider efficient biohydrogen substrates [9]. Lacking lignin is another advantage of using microalgae/cyanobacteria biomass, making it simpler to convert to monosaccharides for fermentation [10]. Cyanobacteria have primarily been studied for their ability to convert solar energy into fixed carbohydrates. Compared to higher plants, cyanobacteria have the higher photosynthetic capacity and faster cell growth rates. Therefore, they can be easily cultivated using only the most essential nutrients, air, water, and light [11].

Oscillatoria sp. is a filamentous cyanobacterium that has been investigated for its potential use in biofuel production [12]. Studies have shown that it has a high carbohydrate level, which can be utilized in biohydrogen synthesis through the process of dark fermentation [6]. Additionally, *Oscillatoria* sp. has been found to be a suitable strain for biohydrogen production due to its high rate of growth and capability to survive in a wide-ranging of environments [13]. Carbohydrates in cyanobacteria are mainly derived from glycogen accumulated in the cytoplasm and various cell wall polysaccharides, which are not easily fermentable by microbes for biohydrogen generation [9]. As a result, various pretreatment methods are being used to break and hydrolyze the intricate cell wall carbohydrates in order to produce simple fermentable sugars, consist of physical (grinding, sonication and pyrolysis), chemical (alkali, acid and thermal), and biological (enzymes) pretreatments [14]. However, the

most effective approach for cyanobacteria has yet to be determined. As a result, several pretreatment protocols have been used with variable degrees of achievement. Pretreatment optimization can help with cost-effective hydrogen production since its eco-friendly, power-saving, and has zero carbon emission. The conversion of cyanobacterial biomass into sustainable biohydrogen by H₂-producing bacteria through dark anaerobic fermentation is getting prominence [15] due to its energy-efficient, environmentally benign, and carbon-neutral properties. It is a talented energy source candidate to substitute traditional fossil fuels, which is advantageous from both an economic and environmental perspective [16]. Most biological H₂ generation activities occur at ambient temperatures and pressure [17]. These milder conditions are better for the environment and save energy.

Recently, scientists have been exploring the use of nanomaterial catalysts as a way to enhance the conversion of cellulosic and lignocellulosic biomass into sugar [18–20]. Nanoparticles have unique physical, chemical, and electrical properties compared to their bulk counterparts. They can be used as catalysts in the fermentation process and have a positive effect on the stability and efficiency of the microorganisms involved in the fermentation process [21–23]. Various types of nanomaterials, such as magnetic, carbon nanotubes, and metal oxide nanoparticles, have been studied for their potential in sustainable bioenergy production [24]. However, few studies have been conducted on the use of nanoparticles to enhance the enzymatic conversion of algal biomass for sugar production in fermentation processes [18].

On the other hand, identifying and isolating hydrogen-producing bacteria is another challenging step in biohydrogen production. Wastewater sludge is one of the rich sources of hydrogen-producing bacteria. This includes isolates from various genera, such as *Clostridium*, *Bacillus*, *Enterobacter* and *Klebsiella*, among others [25]. The enterobacterium species such as *Enterobacter cloacae* and *Klebsiella pneumoniae* were selected from environmental sources and has shown potential for producing biohydrogen from different substrates [25–27].

On the basis above facts, this work aimed to utilize the *Oscillatoria acuminata* biomass as substrate in hydrogen production. Biological pretreatment + Mg-Zn Fe₂O₄ NPs was applied to *Oscillatoria acuminata* biomass for the first time, according to our knowledge, to enhance their soluble and fermentable sugars for rapid bacterial consumption in hydrogen production. The results were compared with thermochemical and biological pretreatments. Biohydrogen production from *Klebsiella pneumoniae*, *Enterobacter cloacae* individually or their coculture were studied to trigger the conversion of cyanobacterial

biomass into biohydrogen. Furthermore, the biohydrogen evolution efficiency was computed in terms of dry mass and reducing sugars.

Results and discussion

Isolation and identification of microalgal species

Oscillatoria was genetically identified using 16S rRNA gene, respectively. The sequence analysis was done with the neighbor-joining algorithm based on the parameter distance (NJ-PD) by aligning the 16S

gene sequence with 16S nucleotide sequences of 16 cyanobacteria species plus four 16S sequences of *Planktothrix agardhii* as an outgroup (Fig. 1). Each *Oscillatoria* sp. formed monophyletic subclades with bootstrap support, ranging from 87 to 100. The sequences were subjected to BLAST homology searches of the 16S sequence, indicating that the closest match was *Oscillatoria acuminata* (Fig. 1). *Oscillatoria* sp showed very high similarity (~98–100%) to *Oscillatoria acuminata* (MK014210, NR_102463, and

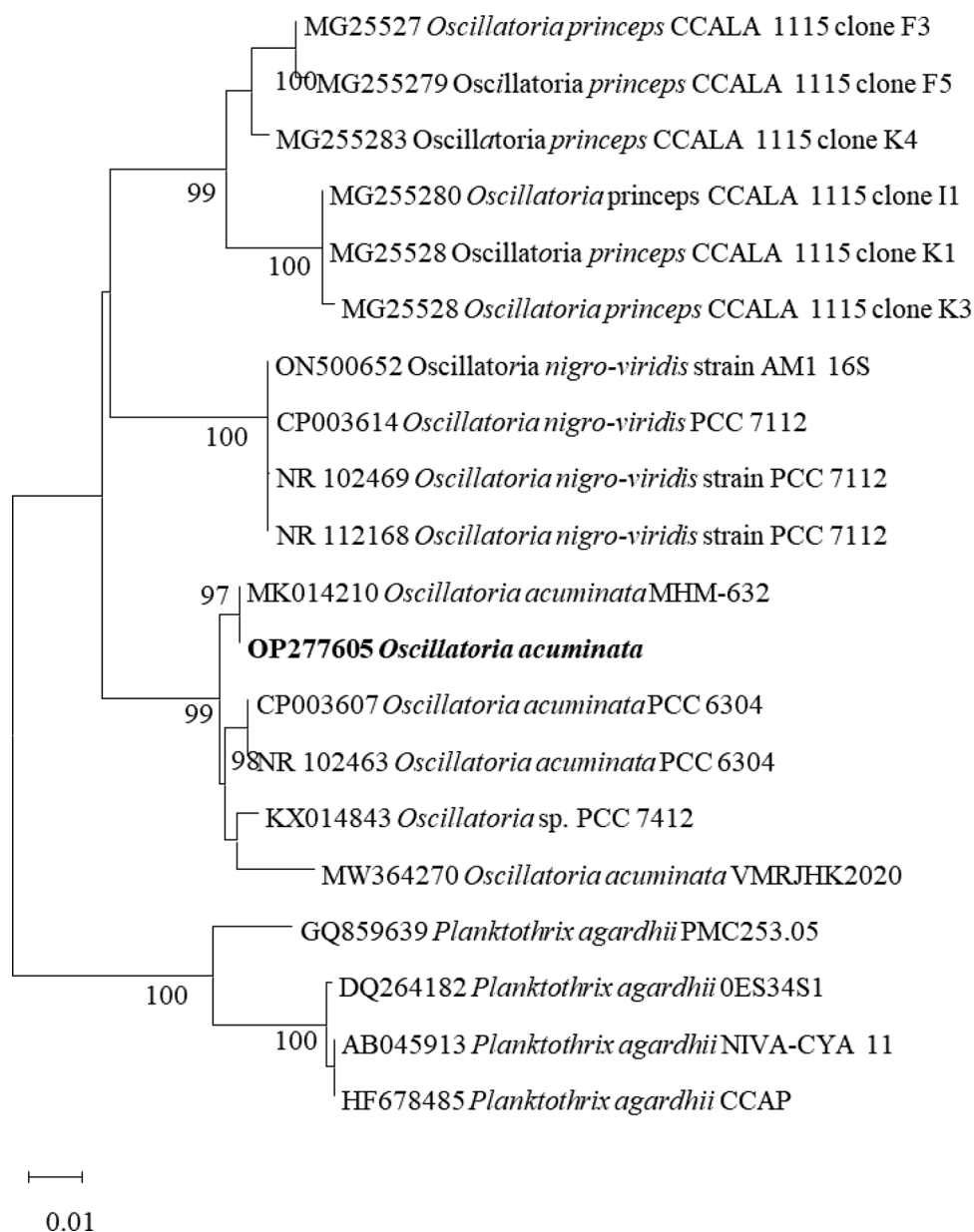


Fig. 1 Neighbor-Joining (NJ) dendrograms showing the isolated *Oscillatoria acuminata* based on 16S rRNA nucleotide sequences, respectively. Bootstrap values higher than 70 are shown below the branches of the trees

CP003607). The sequences of the cyanobacteria have been submitted to Genbank (OP277605).

Estimation of growth and biochemical composition of *Oscillatoria acuminata*

The algal growth was determined by optical density and dry weight. The results in Fig. 2 indicated that the growth curve of *O. acuminata* showed no lag phase. The exponential phase was from zero to the 14th day. These cultivation periods are shorter than those recorded by El-Sheekh et al. [28], who denoted that *O. acuminata* could grow till the 22nd day of cultivation. This difference in biomass may be due to the differences in culture medium, cultivation condition, and metabolic activity [29, 30].

The biochemical composition was estimated at the end of the log growth phase on the 16th day of culture (Table 1). Chl a and carotenoid content extracted from *O. acuminata* recorded maximum value at 16th (18.1 $\mu\text{g/mL}$, 3.3 $\mu\text{g/mL}$ respectively). *O. acuminata* showed the highest carbohydrate content of 237.39 mg/L, while the total protein content was 180.78 mg/L. These results are less or more than those recorded in recent studies [29]. This could be attributed to the difference between the isolates, biomass yield, and growth conditions [31]. Microalgal biomass was harvested on the 16th day for use in further experiments.

Table 1 Metabolic constituents of *O. acuminata*

Biochemical constituents	Contents
Chlorophyll a ($\mu\text{g/mL}$)	18.1 \pm 0.3
Carotenoid ($\mu\text{g/mL}$)	3.3 \pm 0.07
Total soluble protein (mg/L)	180.78 \pm 2.21
Total soluble carbohydrate (mg/L)	237.39 \pm 4.12

Values represent means of three replicates \pm standard error

Influence of different pretreatment methods on biomass hydrolysis

Pretreatment is crucial in releasing fermentable sugars to be used in microbial fermentation.

Thermochemical pretreatment of microalgal biomass

As shown in Fig. 3, the highest value of reducing sugar was recorded at 1.5% H_2SO_4 of 45.34 mg/g dry weight DW, while any increase or decrease in H_2SO_4 concentrations reduces sugar content reduced. Among various acids hydrolysis, Hessami et al. [32] proved that H_2SO_4 is the best hydrolysis acid compared to HCl, HClO_4 and CH_3COOH . Thus, acid hydrolysis using sulphuric was performed in the current study as an efficient, fast, appropriate and cost-effective technique [33]. Furthermore, El-Souod et al. [34] demonstrated that hydrolysis of microalgal biomass using H_2SO_4 pretreatment showed the best results, especially at 1.5%. These results run with Ashour et al. [35], Elshobary et al. [33] and Li et al. [36],

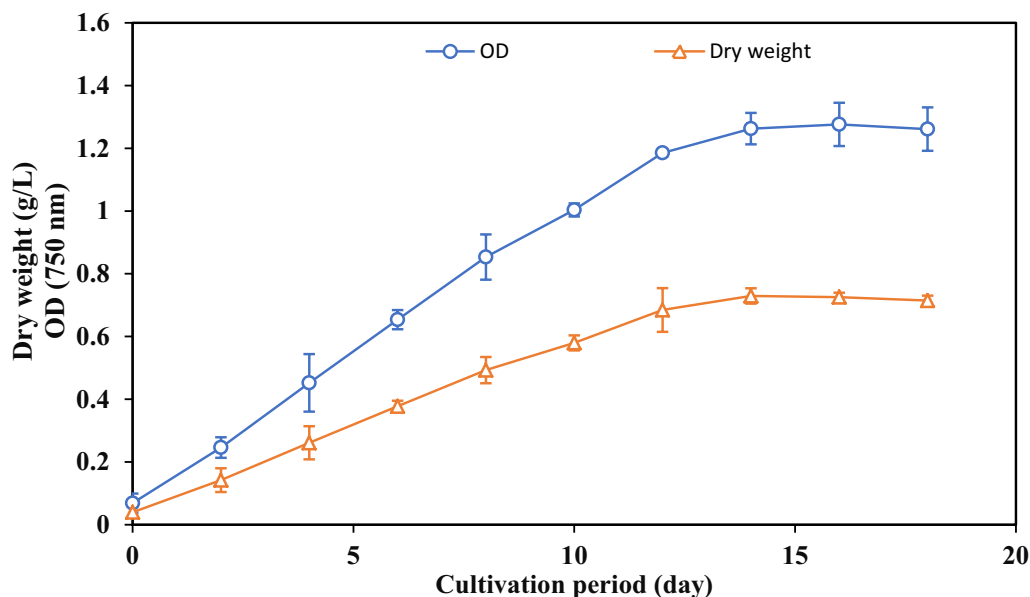


Fig. 2 Growth curve of *O. acuminata* using dry weight and optical density (OD 750)

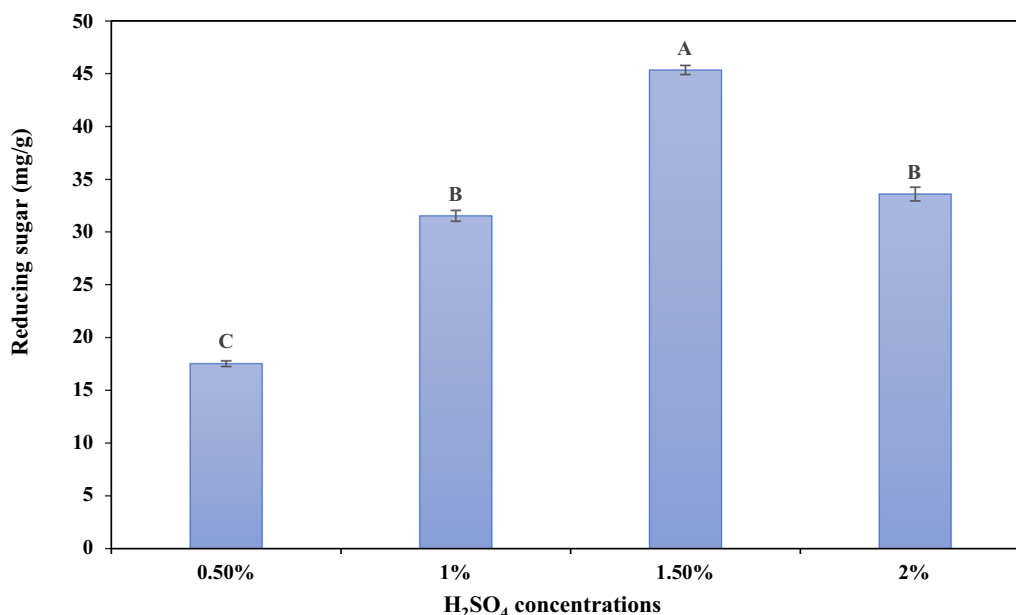


Fig. 3 Effect of different concentrations of acid pretreatments on *O. acuminata* biomass for reducing sugar production. Different capital letters of the plotted series indicate significant differences at $p \leq 0.05$ using Duncan's test

who found that dilute acid pretreatment was extensively used since strong acid would induce the excessive breakdown of the complex material, resulting in a release of fermentable sugars. However, acid pretreatment produces fermentation-inhibiting compounds for example, furfural, hydroxymethylfurfural, and levulinic acid [37]. In contrast, biological pretreatment, such as fungal treatment, may be a further practical alternative than typical acid pretreatment processes [38].

Biological treatment of microalgal biomass

This study studied biological pretreatment as an eco-friendly tool to maximize reducing sugar release, avoid generating fermentation-inhibiting compounds and reduce chemical inputs. Fungi produce several hydrolysis enzymes such as cellulase, filter paper cellulase and β -glucosidase. These enzymes break down the algal cell wall and convert complex polysaccharides to fermentable monosaccharides. *T. harzianum* (OP264067) showed the highest cellulolytic activity compared to 20 isolated fungi [39] and naturally produces hydrolysis enzymes such as cellulase, β -glucosidase and xylanase [40].

Screening of different substrates for cellulolytic activity produced by *T. harzianum* using solid-state fermentation (SSF)

To further increase the hydrolysis process and reducing sugar content, optimization of biological pretreatment was conducted using different substrates (rice straw,

wheat straw, and wheat bran) Fig. 4. Results demonstrated that wheat bran was the most efficient substrate that improved the cellulolytic activity of *T. harzianum* to the maximum. The maximum activities of CMCase, β Gase, Fpase were 1320.57, 940.59 and 402.41 U/g DW substrate, respectively and total cellulolytic activity was 2663.56 U/g DW using wheat bran, followed by rice straw (1582.52 U/g DW), and wheat straw (1345.06 U/g dry weight substrate). Our results agreed with El-Shishtawy et al. [41], who reported that wheat bran substrate enhanced the hydrolysis enzymes, total proteins, and carbohydrates of *T. virens* to the maximum using base pretreated. Moreover, wheat bran revealed its potential as a cheap substrate for more remarkable enzyme synthesis by *Penicillium citrinum* [42]. One unit of FPase, β Gase, and CMCase was described as μ g of reducing sugars produced per minute per gram of substrate dry weight.

Effect of Mg-Zn Fe₂O₄-NPs on the hydrolytic enzymes of *T. harzianum*

Cellulolytic action of *T. harzianum* using wheat bran as substrate was further improved by Mg-Zn Fe₂O₄-NPs as shown in Fig. 5. The results concluded a gradual increase in all cellulolytic activities (CMCase, β Gase, Fpase and total cellulolytic activity) by applying different Mg-Zn Fe₂O₄-NPs concentrations until reaching the maximum activities at 60 ppm of Mg-Zn Fe₂O₄-NPs for CMCCase, β Gase, Fpase (2162.40, 877.65 and 659 U/g respectively) with the highest total cellulolytic activity (4319.37 U/g).

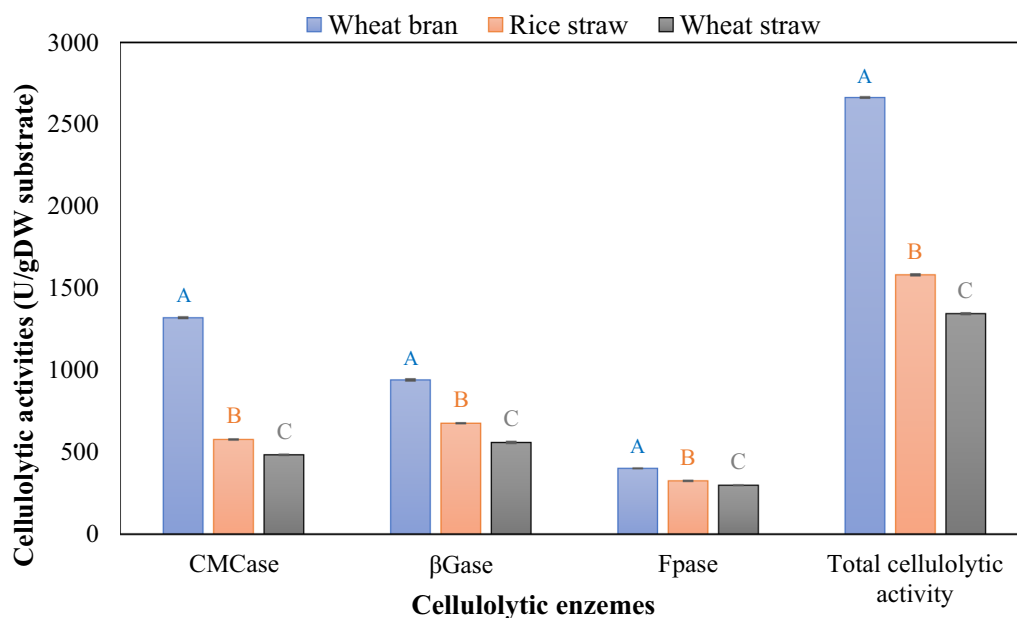


Fig. 4 Screening of different substrates for cellulolytic activity produced by *T. harzianum* using solid-state fermentation (SSF). Different capital letters of the plotted series indicate significant differences at $p \leq 0.05$ using Duncan's test

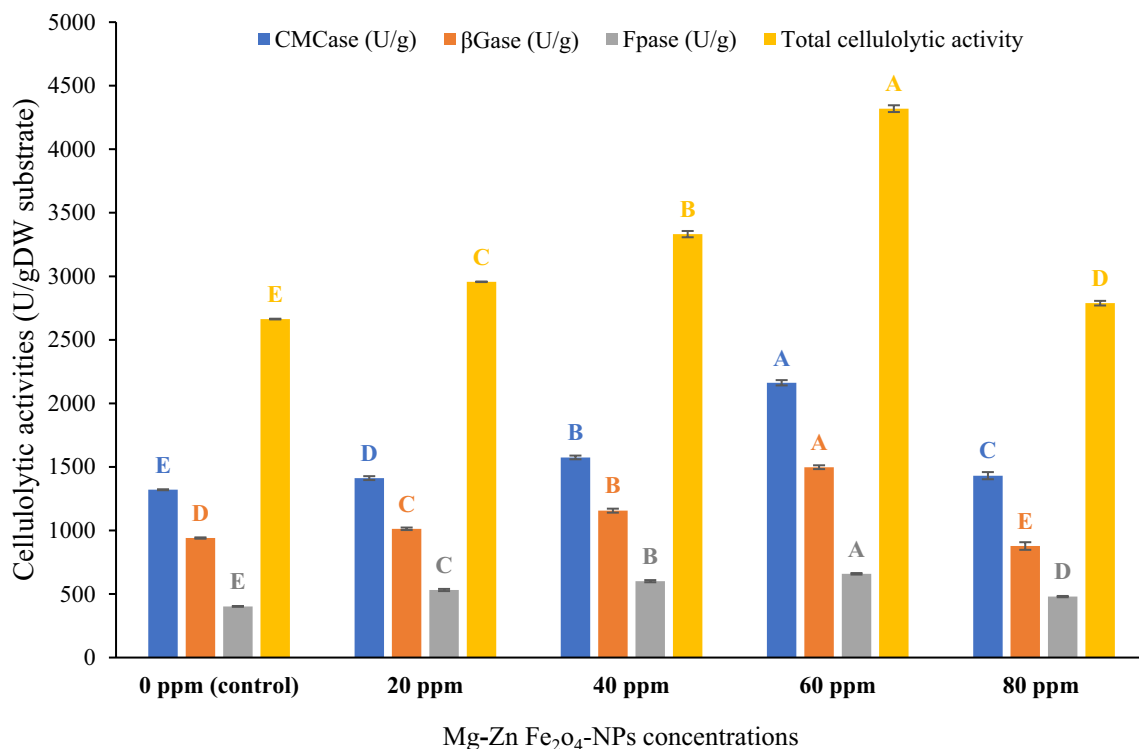


Fig. 5 Effect of Mg-Zn Fe₂O₄-NPs for cellulolytic activity produced by *T. harzianum* Ps-2 using solid-state fermentation (SSF). All data represented means of 3 replicas \pm standard deviation (SD). Different capital letters in each plotted series indicate significant differences at $p \leq 0.05$ using Duncan's test

Interestingly, 60 ppm of Mg-Zn Fe₂O₄-NPs improved the total cellulolytic activity about two times over the untreated control. It has been observed that the presence of metal oxides is essential for the production of cellulase enzymes and growth of microorganisms in fermentative media. This is due to the fact that these micronutrients play a crucial role in the synthesis of cellulase enzymes and microbial growth. Therefore, by incorporating Mg-Zn Fe₂O₄-NPs as a catalyst, it enhanced the production of cellulase enzymes and bio-hydrogen [20]. Moreover, the stability of enzymes can be significantly improved through protein adsorption on nanomaterials, due to the unique properties provided by high surface area to volume ratios [43]. Furthermore, the high surface area of nanoparticles offers an efficient matrix for immobilizing enzymes, resulting in enhanced stability. The large surface area of these materials allows for multiple points of attachment for enzyme particles, which prevents protein unfolding and ultimately leads to improved enzyme stability [44]. Srivastava et al. recorded that nickel ferrite nanoparticles stimulated the yield of total cellulase enzyme using remaining cyanobacteria biomass of *Lyngbya limnetica* as feedstock [18]. Asar et al. reported a comparable increase in cellulase and sugar yield following the application of iron oxide magnetic nanocomposites [45].

Effect of enzyme dose and incubation duration on cyanobacterial biomass

One of the most common and straightforward experiments used to improve the fermentation process is single-factor optimization [46, 47]. Effect of enzyme dose and incubation duration were determined and optimized by a series of single-factor experiments to provide optimal conditions for the fermentation process. The results illustrated in Fig. 6 showed that the highest yield (106.48 mg/g) of reducing sugar and cellulolytic activity (5958.50 U/g) were recorded at 1:2 crude enzyme: algal suspension (33%) concentration after 12 h. Cellulolytic activity at an enzyme concentration of 33% increased by 52.31%. These results may be explained by increasing algal suspension increases the substrate and available carbon source for the enzyme activity. In this context, Vishwakarma and Malik investigated the enzymatic pretreatment effects using crude enzymes from *T. reesei* increased by twofold in protein efflux and a 41% increase in released sugars after 12 h of enzymatic pretreatment at 33% (v/v) enzyme concentration [48].

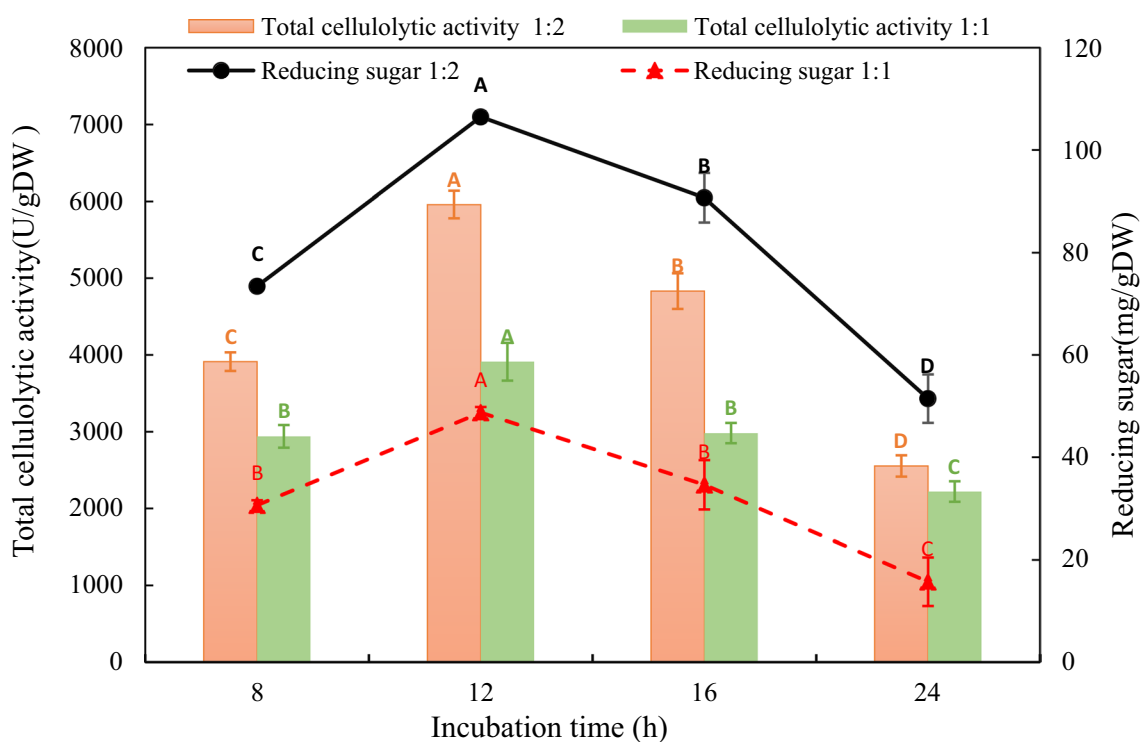


Fig. 6 Effect of enzyme dosage and incubation time on biodegradation of *O. acuminata* biomass. All data represented means of 3 replicas ± standard deviation (SD). Different capital letters in each plotted series indicate significant differences at p ≤ 0.05 using Duncan's test

Cellulolytic activity and reducing sugar in the presence of Mg-Zn Fe₂O₄-NPs by solid state fermentation

Optimized conditions of 1:2 crude enzyme: algal suspension at 12 h incubation were subjected to Mg-Zn Fe₂O₄-NPs to maximize the cellulolytic activity and reducing sugar content of *O. acuminata* biomass. As a result, Mg-Zn Fe₂O₄-NPs significantly induced the production of reducing sugar and cellulolytic activity by 20.1% (7158.50 U/g) and 1.16-fold of reducing sugar (230.48 mg/g, 23.05 g/L) compared to biological pretreatment without NPs.

Fewer studies have been conducted on the use of nanoparticles to treat enzymatic conversion of biomass for sugar production, but the results of this study showed a higher production of sugar and higher cellulolytic activity compared to previous research. For example, Srivastava et al. recorded enhanced cellulolytic activity to 222 U/g by using nickel ferrite nanoparticles using residual biomass of *Lyngbya limnetica* [18]. Zanuso et al. obtained 21.84 g/L reducing sugar production using corn cob biomass using magnetic nanoparticles [49], and Jiang et al. showed an improvement in sugar production using corn stalk with the use of cellulase enzyme immobilized on nanocomposite compared to using the crude enzyme [50]. It is important to note that the type and form of magnetic carboxymethyl chitosan/calcium alginate–cellulase nanomaterials used can greatly impact the efficiency of hydrolysis enzymes, along with the type of fungal strain used. As previously discussed, the type and form of nanomaterials have a significant impact on the effectiveness of enzymes, in addition to fungal species used.

Fourier Transform Infrared Spectroscopy (FTIR) of the algal biomass before and after pretreatment

FTIR was used to demonstrate the structural and chemical variations in different pretreatments (chemical, biological, and biological pretreatment + Mg-Zn Fe₂O₄-NPs) using *O. Acuminata* biomass. The Hydrogen bond band at 3600–3250 cm⁻¹ was diminished after the hydrolysis due to the destruction of many H-bonds in the cellulose molecules [51]. Substantial reduction in the intensity at 3600–3250 cm⁻¹ in biological + Mg-Zn Fe₂O₄-NPs pretreatment, indicating the breaking down of hemicellulose by cracking of H-bond in the amorphous cellulose [52, 53]. Variations in band intensity and position may imply a reduction in structural component concentration as well as the development of different kinds of groups from free radical groups created during treatments [54]. The expansion of the band also shows the bond's weakening as a result of pretreatment. Because these peaks reflect proteins, secondary amines (proteins, lipids), saccharides, and carbohydrates, a drop in intensity correlates to

a reduction in their concentration. The peak at 2860 cm⁻¹ was nearly gone after biological treatment, indicating that the carbohydrate and lipid complexes had been broken down [55]. The functional groups of methylene (-CH₂-), methyl (-CH₃), and glycosidic bond dominated the spectrum area at 1460–1160 cm⁻¹. These groups are extensively dispersed and generated in numerous monosaccharides of the hemicellulose molecule, such as xylose, arabinose, and mannose. [53, 56]. The glycosidic link (C–O–C) breaking down in amorphous cellulose causes an obvious vibration at wavenumbers of 600–1050 cm⁻¹. The intensities of the typical cellulose peaks were found to diminish after treatments (Allard and Templier, 2001). The shift in peak intensity at wavenumbers 700–600 cm⁻¹ was related to the cis–trans structural alteration in the cell wall carbohydrates during biomass processing. The band at 600–900 cm⁻¹ was ascribed to the vibration of ether groups or glycosidic bonds, which were the primary connections in polysaccharide compounds and pectin [57]. These results verified that Mg-Zn Fe₂O₄-NPs enhanced the efficiency of biological pretreatment of *O. acuminata* biomass by sequentially cracking the cell wall structural components (Fig. 7).

Scanning Electron Microscopic (SEM) analysis of the cyanobacterial biomass before and after treatment

In order to get insights into the structural and morphological variations in *O. acuminata* biomass during pretreatments (thermochemical, biological, and biological pretreatment + Mg-Zn Fe₂O₄-NPs). SEM microscopy analysis was used. Figure 8 reveals that the untreated biomass had a normal, smooth, and compact surface structure without degradation (Fig. 8A). After chemical treatment, the cell wall was partially broken (Fig. 8B). In biological treatment, obvious damage observed, resulting in exposure of the inner structure (Fig. 8C) [58]. The structure and integrity of *O. acuminata* cell walls might be efficiently disrupted with biological (fungal) pretreatment. The structure was utterly damaged after applying the biological pretreatment enhanced by Mg-Zn Fe₂O₄-NPs. This biomass treatment led to severe cell morphology alterations, including severe cell breaking and visible cellular debris (Fig. 8D) [59].

Biohydrogen production

Isolation and purification of biohydrogen-producing bacteria

Two bacterial species were isolated from sewage sludge. Biochemical characterizations were performed using Bergey's Bacteriology System to confirm that these isolates belonged to the Enterobacteriaceae family and were identified as *Klebsiella pneumonia* and *Enterobacter cloacae*. In addition, a phylogenetic tree was built

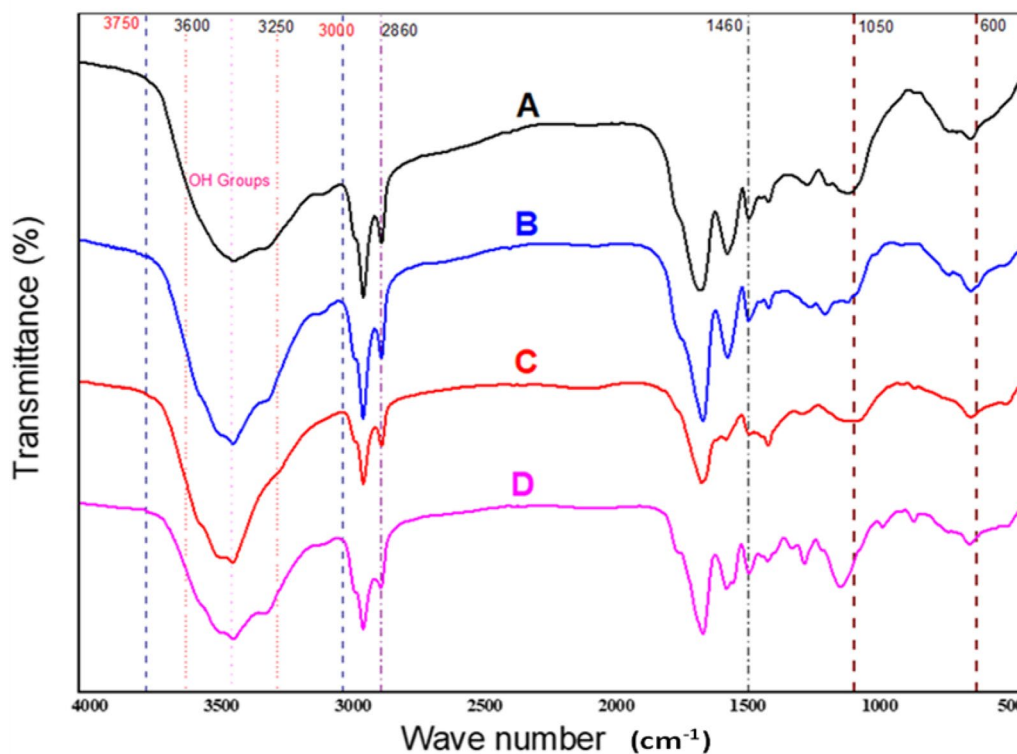


Fig. 7 The diagnostic fingerprint regions of the FT-IR spectra of raw and pretreated *O. acuminata* biomass. A, untreated biomass; B, Chemical pretreatment; C, Biological pretreatment, and D, Biological pretreatment enhanced by Mg-Zn Fe₂O₄-NPs

using the 16S rRNA gene sequence analysis to verify their taxonomic position. For the *Enterobacter cloacae*, the sequence analysis was accomplished with the neighbor-joining algorithm based on the parameter distance (NJ-PD) by aligning the 16S rRNA gene with 16S nucleotide sequences of 26 bacteria species plus five 16S rRNA sequences of *Escherichia coli* as an outgroup (Fig. 9A). These sequences showed identical similarity (100%) to *Enterobacter cloacae* (Genbank ON422258, KX036855, and KJ210328). Therefore, the isolated *Enterobacter cloacae* sequence was banked in the Genbank database under the accession number OP277604.

On the other hand, the *K. pneumoniae* sequences were subjected to BLAST homology searches of the 16S sequence, indicating that the closest match was *K. pneumoniae* (Fig. 9B). The phylogenetic tree comprises 20 sequences of *Klebsiella* sp. and two *Escherichia coli* 16S sequences as an outgroup. *Klebsiella* sp. sequences showed high similarity (~99%) to *Klebsiella pneumoniae* (Genbank CP063925, MT226611 and CP045641) that were grouped in the subclade of the first clade with 86 bootstraps. Therefore, the isolated *K. pneumoniae* sequence was banked in the Genbank database under the accession number OP277603.

Biohydrogen production using hydrolysate of *O. acuminata* by different treatments

Chemical pretreatment

The cumulative biohydrogen production from *K. pneumoniae* and *E. cloacae* as well as their coculture showed significant differences by increasing incubation periods ($p < 0.001$), as illustrated in Table 2. Biohydrogen production from *K. pneumoniae* using thermochemical pretreatment hydrolysate of *O. acuminata* (1022 mLH₂/L) was higher than *E. cloacae* (813 mLH₂/L). The obtained results are in harmony with that detected by Ramu et al. [60], who demonstrated that *K. pneumoniae*-FA2 showed the maximum yield of biohydrogen (1094 mLH₂/L) using food wastewater as a feedstock. The efficiency of *K. pneumoniae* was due to its greater ability to decompose dissolved sugars as a carbon source to generate biohydrogen. While the coculture of *K. pneumoniae* and *E. cloacae* showed superior hydrogen production (1520 mLH₂/L) with an increase of 48% and 53% compared to the monoculture of *K. pneumoniae* and *E. cloacae*, respectively. The same trend was observed using glucose (15 g/L) as the standard substrate.

Moreover, the fermentation process was completed within 72 h in monoculture with significant differences at different incubation periods (*K. pneumoniae*:

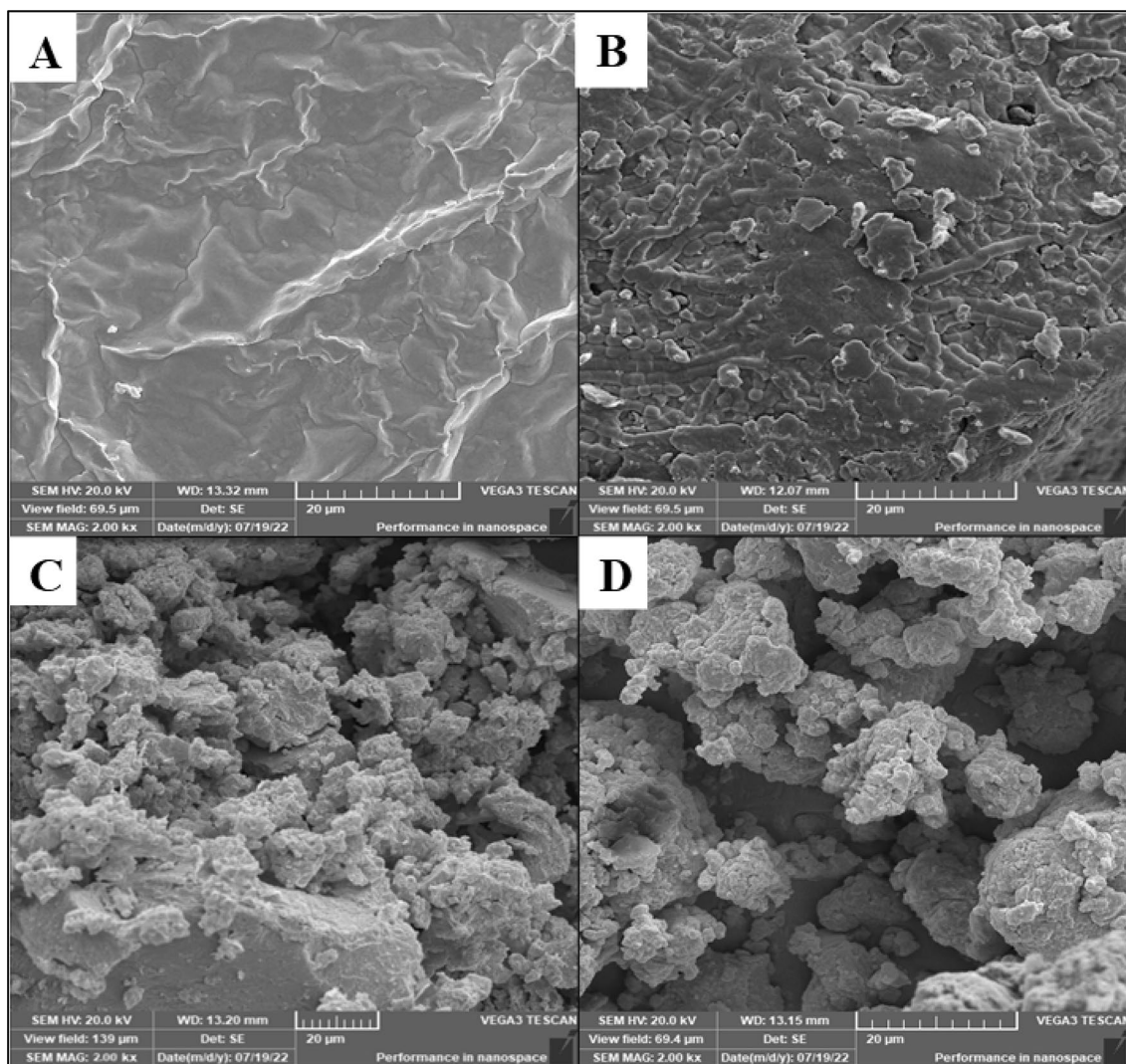


Fig. 8 Scanning Electron Microscopy (SEM) observation of *O. acuminata* biomass at 2000 × magnification. Where, **A**, untreated biomass; **B**, Chemical pretreatment; **C**, Biological pretreatment and **D**, Biological pretreatment enhanced by Mg-Zn Fe₂O₄-NPs

$F=22,145.98$, $df=5$, $p<0.001$; *E. cloacae*: $F=653.23$, $df=5$, $p<0.001$), while the coculture fermentation was achieved in only 48 h with a significant difference at different fermentation periods ($F=1563.4$, $df=3$, $p<0.01$) and generated a superior hydrogen evolution efficiency, hydrogen production, and rate hydrogen yield. Analogous results were obtained by Laxman Pachapur et al., who stated that coculture enhances H₂ production compared to a single bacterial culture [61]. Coculture offers synergistic effects with higher H₂ yield than monoculture [62], requiring less fermentation period and supplying more H₂ [63, 64]. The coculture system works in tandem, guaranteeing process stability and improved performance than monocultures, as well as having overcome the limitations of axenic cultures with economic

and methodological advantages over enzymatically hydrolyzed cellulose by eliminating the use of reductants during H₂ production [65–67]. In addition, the coculture system decreases the incubation time from 3 days to almost 2 days, allowing for additional runs throughout the year and lowering the total cost of H₂ generation. In coculture systems, predetermined microbial strains execute complicated activities such as substrate hydrolysis, metabolism exchange, simultaneous substrate consumption and working on several substrates while lowering the working time and releasing greater hydrogen than in monoculture systems [68]. However, chemical pretreatment was insufficient to release all reducing sugars in *O. acuminata* biomass and may generate compounds that inhibit biohydrogen fermentation. Consequently,

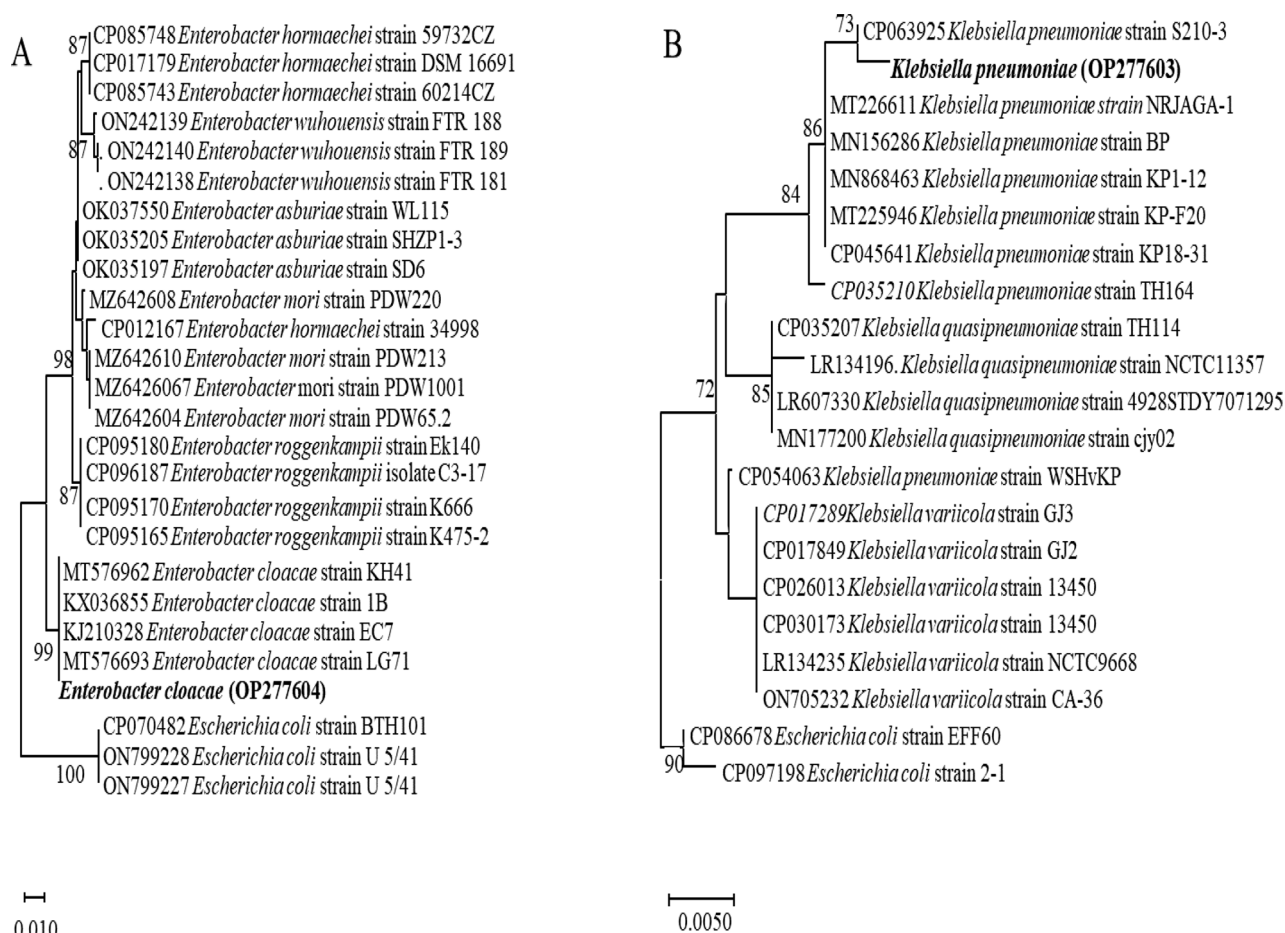


Fig. 9 Neighbor-joining (NJ) phylogenetic tree for *E. cloacae* (A) and *K. pneumoniae* (B) based on 16S nucleotide sequences. Bootstrap values greater than 70 are shown. The identified species in this study were marked in bold

Table 2 Biohydrogen production (mH₂/L) from *K. pneumoniae*, *E. cloacae* and coculture using thermochemical hydrolysate of *O. acuminata*

Cultures	<i>K. pneumoniae</i>		<i>E. cloacae</i>		Coculture	
	Glucose	<i>O. acuminata</i>	Glucose	<i>O. acuminata</i>	Glucose	<i>O. acuminata</i>
12	372 ± 9.62	350 ± 9.62	238 ± 9.62	216 ± 9.62	500 ± 20.45	400 ± 18.56
24	578 ± 25.45	498 ± 25.45	422 ± 16.66	344 ± 16.66	960 ± 30.25	890 ± 25.12
36	655 ± 9.62	583 ± 16.66	486 ± 16.66	433 ± 16.66	1160 ± 32.89	1250 ± 19.34
48	927 ± 9.62	855 ± 9.62	612 ± 9.62	572 ± 25.45	1300 ± 20.56	1520 ± 33.5
60	983 ± 16.66	933 ± 16.66	684 ± 16.66	683 ± 25.45	–	–
72	1046 ± 16.66	1022 ± 9.62	835 ± 25.45	813 ± 9.62	–	–
F-value	1254.45*	22145.98*	1365.98*	653.23*	2653.2*	1563.4*

Values represent means of three replicates ± standard error; * indicate significant differences (p ≤ 0.05)

biological and biological treatment + Mg-Zn Fe₂O₄ NPs were used to enhance hydrogen production using the coculture of *K. pneumoniae* and *E. cloacae*.

Biological and biological pretreatment + Mg-Zn Fe₂O₄ NPs treatment

Biological pretreatment of microalgal biomass was used to augment their fermentable contents for

Table 3 Biohydrogen production (mLH₂/L) from coculture of *K. pneumoniae* and *E. cloacae* using hydrolysate of *O. acuminata* by biological treatment

Incubation period (h)	Glucose	Biological treatment	Biological treatment + Mg-Zn Fe ₂ O ₄ NPs
12	500 ± 20.45	500 ± 22.65	590 ± 36.45
24	960 ± 30.25	1765 ± 23.25	2214 ± 70.21
36	1160 ± 32.89	2134 ± 37.25	2954 ± 66.3
48	1300 ± 20.56	2645 ± 31.02	3254 ± 36.54
F-value	2653.2*	1632.6*	9561*

Values represent means of three replicates ± standard error; * indicate significant differences (p ≤ 0.05)

hydrogen-producing bacteria. As a result, biohydrogen production from mixed cultures was increased to 2645 mLH₂/L in *O. acuminata* at 48 h with significant differences among fermentation periods (F = 1632.6, df = 3, p < 0.01) (Table 3) representing 74% more than chemical pretreatment. This may be because enzymes of biological pretreatments contain amino acids rich in nitrogen that maintains proper nutrient levels throughout fermentation, enhance the growth and protect fermentative microorganisms from osmotic stress [69].

Biological treatment + Mg-Zn Fe₂O₄ NPs significantly induced hydrogen production rates compared to the other pretreatments. Accumulative hydrogen production of the coculture was enhanced to attain 3254 mLH₂/L

at 48 h with substantial differences amongst fermentation periods (F = 9561, df = 3, p < 0.001) (Table 3). These amounts represent 1.14-fold when compared with chemical treatment, as shown in Fig. 10. This yield was the highest amount developed among all applied treatments. Abdel-Kader et al. observed that hydrogen production of the mixed cultures of bacterial strain (*Rhodobacter* sp, *Rhodospseudomonas palustris*) was improved to attain 4700 mLH₂/L culture [14]. Srivastava et al. recorded an increase in hydrogen yield to 1820 mLH₂/L via *Bacillus subtilis* PF_1 by using NiFe₂O₄ NPs treated cyanobacteria biomass [18]. Moreover, the remaining nanoparticles in the biological pretreatment hydrolysate may have a crucial role in enhancing the hydrogen accumulation. The iron and its oxide NPs clearly activate the main enzymes of hydrogen generation and boost their activities by supplying iron for synthesis and maintaining the essential enzymes' molecular structure [70–72]. Moreover, the use of nanoparticles in stabilizing enzymes has been shown to increase sugar production and subsequently, biohydrogen production in a shorter time, thus speeding up the fermentation process [73].

Hydrogen evolution efficiency

Hydrogen evolution efficiency (HE) was estimated as attributed to reducing sugar (RS) (consumed sugar) as mL H₂/g RS and hydrogen yield (mL H₂/g DW) as shown in Table 4. The maximum HE value)216.9 mL H₂/g RS,(hydrogen yield (92.9 mL H₂/g Dw, 4.15 mmol/g DW) and

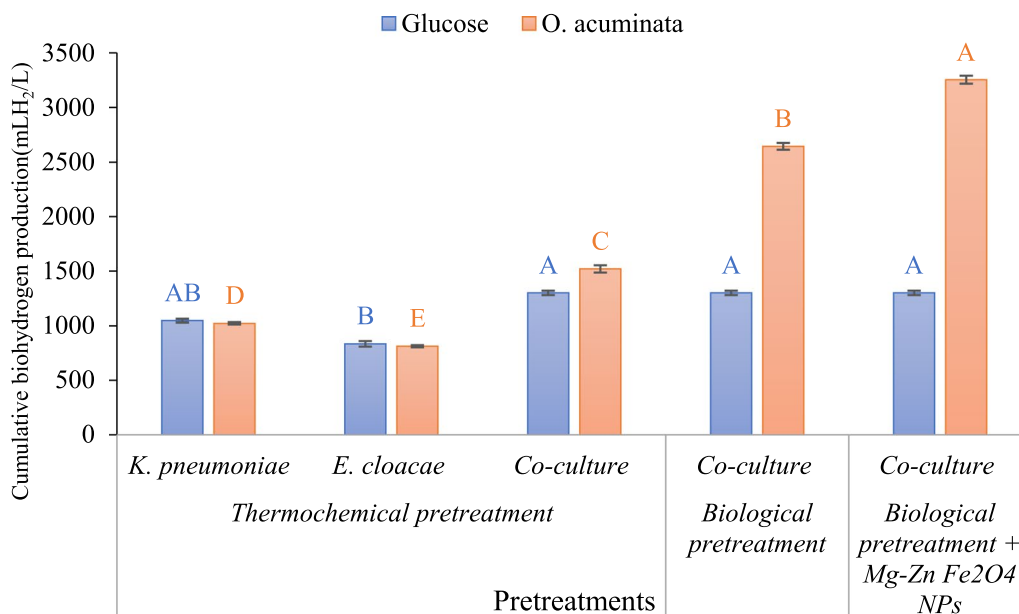


Fig. 10 Cumulative biohydrogen production after 48 h from *K. pneumoniae*, *E. cloacae* and their coculture using different hydrolysates of *O. acuminata* compared to glucose standard. Each value represents the mean value of three independent replicates. Different capital letters in each plotted series indicate significant differences at p ≤ 0.05 using Duncan's test

Table 4 Hydrogen evolution efficiency (mLH₂/g RS), hydrogen yield (mL/g DW) and hydrogen rate (mL/L/h) from *K. pneumoniae* and *E. cloacae* and their mixed coculture using hydrolysates *O. acuminata* of by different treatments

Cultures	<i>K. pneumoniae</i>		<i>E. cloacae</i>		coculture			
	Glucose (15 g/L)	Thermochemical pretreated <i>O. acuminata</i> (35 g/L)	Glucose (15 g/L)	Thermochemical pretreated <i>O. acuminata</i> (35 g/L)	Glucose (15 g/L)	Thermochemical pretreated <i>O. acuminata</i> (35 g/L)	Biological pretreated <i>O. acuminata</i> (35 g/L)	Biological treated + NPs <i>O. acuminata</i> (35 g/L)
Initial sugar (g/L)	15 ± 0.47	16 ± 0.57	15 ± 0.47	16 ± 0.57	15 ± 0.47	16 ± 0.57	31 ± 0.54	45 ± 1.36
Residual sugar (g/L)	3.1 ± 0.17	5.2 ± 0.27	3.2 ± 0.12	5.2 ± 0.65	2.6 ± 0.12	4.6 ± 0.21	17 ± 0.63	29.34 ± 1.07
Consumed sugar (g/L)	11.9 ± 0.13	10.8 ± 0.63	11.8 ± 0.39	10.8 ± 0.64	12.4 ± 0.8	11.4 ± 0.76	14 ± 0.52	15.66 ± 0.9
Total hydrogen (mL H ₂ /g RS)	87.9 ± 2.3	94.6 ± 3.28	70.8 ± 1.6	75.3 ± 2.5	104.8 ± 3.6	133.3 ± 4.2	188.9 ± 5.3	216.9 ± 4.69
Hydrogen yield (mL H ₂ /g DW)	69.8 ± 1.2	29.2 ± 0.8	55.7 ± 2.3	23.2 ± 1.7	86.7 ± 2.2	43.4 ± 1.6	75.6 ± 1.6	92.9 ± 1.68
hydrogen rate (mLH ₂ /L/h)	14.52 ± 0.6	14.19 ± 0.91	11.5 ± 0.62	11.2 ± 0.25	27.08 ± 1.03	31.66 ± 2.01	55.10 ± 2.1	67.7 ± 3.4

Values represent means of three replicates ± standard error

hydrogen production rate (67.7 mL/L/h) was obtained from biological treatment + Mg-Zn Fe₂O₄ NPs of *O. acuminata* using co-cultures bacterial culture with an increase of 1.62, 1.14 and 1.13-fold, respectively compared to thermochemical pretreatment of coculture. These findings are in close agreement with that presented by Wieczorek et al., who observed that hydrogen yield differs significantly in the range of 11–135 mL H₂/g from pretreated biological microalgae [74]. Wang and Yin, indicated that hydrogen yield by anaerobic sludge from microalgae pretreated by the combined methods varies in the range of 33.5–92.68 mL H₂/g [75].

Conclusions

Based on the current results, it can be concluded that biological pretreatment maximizes reducing sugar release, avoids generating fermentation-inhibiting compounds and reduce chemical inputs compared to thermochemical pretreatments. Mg-Zn Fe₂O₄-NPs enhanced *Trichoderma harzianum* cellulolytic activity to give the bacteria with the largest easily fermentable sugar (230.48 mg/g) to produce the highest H₂ evolution among other pretreatments owing to their high hydrolase content and therefore ability to hydrolyze *O. acuminata* biomass. Furthermore, the coculture of the two studied bacteria, *K. pneumoniae* and *E. cloacae*, produced more hydrogen (3254 mLH₂/L), reflecting synergistic consumption of available resources. Therefore, biological pretreatment + Mg-Zn

Fe₂O₄-NPs and coculture dark fermentation are helpful for biohydrogen production using microalgae biomass.

Material and methods

Materials

All reagents and chemicals used in the current study were of analytical grade. They were purchased from the Sinopharm Chemical Reagent Co., Ltd. (Huangpu, Shanghai, China) or Sigma-Aldrich Chemical Co. (St. Louis, MO, USA).

Nano ferrite nanoparticles in the chemical formula Mg_{1-x}Zn_xFe₂O₄ (x=0.1) were kindly provided by Dr. Ahmed Henaish, Physics Department, Faculty of Science, Tanta University, Tanta, Egypt. Mg-Zn Fe₂O₄-NPs were synthesized using mechanical ball milling method [76].

Microalgal species and culture media

Oscillatoria sp. isolated from channels and sewage in Gharbia Governorate was used as model microorganisms in the present study. The sub-culturing method was used to isolate and purify axenic cultures to obtain axenic cultures. The cyanophyte was identified morphologically and authenticated according to standard references [77] and AlgaeBase digital resources [78].

Culture technique for microalgal species

Oscillatoria sp. was inoculated (OD=0.06) into 500 mL Erlenmeyer flasks containing autoclaved 250 mL of the BG11 (Blue-Green algae) medium [79]. The culture was

sparkling by air pumps and incubated at 25 ± 2 °C under continuous daylight fluorescent tubes giving a light intensity of $80 \mu\text{mol. Photon m}^{-2} \text{s}^{-1}$ [80].

Molecular genetic characterization of microalgal species

Oscillatoria sp. was genetically identified based on 16S rRNA. Total genomic DNA was extracted and purified from the isolated species using the GeneJet Genomic DNA purification Mini Kit (Thermo Scientific) following the manufacturer's procedure. A CreaCon thermal cyclers was used to do the amplicon (Holand). Green taq (DreamTaq) master mix (Thermo Scientific) was employed as directed by the manufacturer for gene amplification. 16S rRNA primer was applied to amplify cyanobacterial 16S rRNA region using universal forward primer 27F (5'-AGAGTTTGATCCTGGCTCAG-3') and 1492R (5'-CTACGGCTACCTTGTTCAG-3'). The thermal cyclers conditions were initiated with denaturation for 3 min at 94 °C followed by 35 incubation cycles, each consisting of 1 min denaturation at 94 °C, 1.5 min annealing at 59 °C, 2 min elongation at 72 °C and a final 5 min elongation at 72 °C [81, 82].

PCR products were purified via Gene JET PCR Purification Kit (Thermo Scientific). ABI PRISM[®] 3100 Genetic Analyzer was applied for PCR products and operated by Macrogen In. Seal, Korea. To identify the closely related species, the purified products were sequenced and aligned with various 16S rRNA get through the nBLAST search (<http://www.ncbi.nlm.nih.gov/blast>). Clustal W with the default settings of MEGA 11 software [83] was used to align the sequences. In addition, MEGA 11 software was used to generate a dendrogram based on the neighbor-joining (NJ) technique [84] using the parameter distance (PD) [85].

Estimation of growth, photosynthetic pigments, total soluble protein and carbohydrate content of microalgal species

The growth curve of each microalgal species was detected by optical density (OD 750 nm) and dry weight day after day for 3 weeks [86]. Protein content was determined according to the Bradford method [87]. Total carbohydrates were estimated by spectrophotometry using phenol-sulphuric acid against glucose standard [88] according the procedures of the previous studies [81, 89].

Microalgal biomass pretreatments

Microalgal biomass was pretreatment by thermochemical, biological, and biological + Mg-Zn Fe₂O₄-NPs before being used as a substrate for fermentation.

Thermochemical pretreatment

In this pretreatment, different concentrations of H₂SO₄ (0.5%, 1%, 1.5%, 2%) with a ratio of 10 ml solution/1 gm microalgal biomass were used [90]. This pretreatment saccharified the complex sugar in the algal biomass to simple. Entire hydrolysates were neutralized with 1 M NaOH to be used in dark fermentation.

Biological treatment

Trichoderma harzianum Ps-2 of high cellulolytic activity, according to our previous study [39] was used as the source of hydrolytic enzymes. First, it was identified using the ITS region and submitted in the gene bank (Accession no: OP264067) (Additional file 1: Figure S1). Then, two successive steps were performed to improve the cellulolytic activity of this fungi. Firstly, different substrates of agricultural wastes (wheat straw, rice straw, and wheat bran) were used in solid-state fermentation (SSF). Then, five grams of each dry, milled (0.5–1 cm) substrate were mixed with 2.5 g yeast extract/L deionised water, with the moisture level maintained at 60%. Next, a fungal spore suspension (10^6 cells/mL) was aseptically inoculated in flasks (5%; w/v of the substrate) and incubated at 30 °C for 5 days [91].

Secondly, different concentrations of Mg-Zn Fe₂O₄-NPs (20 to 80 ppm) were applied for the suitable agriculture waste substrate in SSF under the same condition. The crude enzymes were extracted by adding Na₃C₆H₅O₇ buffer (50 mL, 0.5 M, pH 4.8), which contained 0.1% Tween 80 and incubated in a shaker for 1 h at 160 rpm. The entire contents were centrifuged at 6000 rpm at 4 °C for 20 min. The supernatant of the crude enzymes was analyzed for cellulolytic enzymes. The optimum substrate was set for the following experiments.

Effect of enzyme dose and incubation duration of cyanobacterial biomass

The crude enzyme mix was homogenized with the cyanobacterial suspension (0.3 g in 10 mL) in two ratios (1:1 and 1:2; crude enzyme: algal suspension) to make the final concentration of the crude enzyme 50% and 33% (v/v). The efficacy of the enzymatic activity was estimated after 1 h and 24 h of incubation.

Enzyme action on cyanobacterial biomass

The enzyme action was studied by estimating the reducing sugars, Fourier Transform Infrared Spectroscopy (FTIR), and scanning electron microscope (SEM) analysis

to visualize the morphologic changes in the biomass texture.

Fourier Transform Infrared Spectroscopy (FTIR)

The FT-IR spectrum analysis was conducted using a Vertex 80v powder FT-IR spectrometer (FTIR Bruker) (model, TENSOR27). Two mg of dried *Oscillatoria* biomass (treated and untreated) samples were mixed well with 200 mg of potassium bromide to make pressed discs for FT-IR measurement in the frequency range of 500–4000 cm^{-1} [92].

Scanning electron microscopic (SEM) analysis

SEM analysis was used to analyze the morphological and micro-structural variations of the treated and untreated samples using SEM (Tescan vega 3 SBU, Czech Republic) at an accelerating voltage of 220 keV. The samples were displayed on aluminum microscopy stubs using carbon tape, then covered with a thin layer of gold (Au) for 120 s using Quorum technique Ltd, sputter coater (Q150t, England) [93].

Biohydrogen production

Isolation and identification of biohydrogen-producing bacteria

The bacterial strains were isolated from Tanta, Egypt's wastewater treatment plant (Elmorashaha). The sludge was blended with sterile distilled water before being dispersed onto sterilized nutrient agar plates and incubated at 37 °C in a N₂-flushed anaerobic incubator. The isolated colonies were then inoculated in a cuvette with a Durham tube and cultivated in an anaerobic incubator. The Durham tube would detect evolved gas instantly. The syringe and gas chromatography were used to quantify the volume and composite of evolved gas within the syringe, and the strains with the greatest hydrogen generation yield or rate were chosen [94]. The bacterial isolates were morphologically and biochemically characterized according to Bergey's manual of systematic bacteriology [95]. Also, these isolated bacteria were further identified by 16S rRNA sequencing according to "Influence of different pretreatment methods on biomass hydrolysis" Section.

Experimental design of biohydrogen production

Biohydrogen production was carried out via dark batch fermentation of hydrolysate of the three pretreatments of microalgal biomass (thermochemical, biological, and biological + Mg-Zn Fe₂O₄-NPs) using the two isolated bacteria individually or their coculture. Batch experiments

were performed in 100 mL bottles containing the autoclaved anaerobic medium with 10% V/V of pre-enriched pure bacterial culture. The bottles were sealed with sterilized air-tight rubber caps and parafilm, then purged with nitrogen gas for 3 min to drop the dissolved oxygen concentration down to zero. The bottles capped with rubber stoppers were stirred using the magnetic stirrer plate to help evolve hydrogen [14]. The heater and temperature probe of the magnetic stirrer held the water temperature constant at 37 °C. The gas was trapped in a water inverted cylinder and connected with 2 M NaOH solution to absorb CO₂ produced during fermentation. Hydrogen yield was measured by the liquid displacement technique.

Determination of the produced biohydrogen by gas chromatography (GC)

The evolved biohydrogen gas was determined by gas chromatograph apparatus (Thermo Scientific TRACE GC Ultra) equipped with a thermal conductivity detector (TCD) and Shin Carbon packed column (ST 80/100 2 m, 2 mm ID). Argon was used as carrier gas. For each pretreatment, triplicates were performed, and the average values were taken as the final result. A control test was performed using a fermentative medium containing glucose. An additional blank assay with only an anaerobic medium without any substrate or inoculum also acted as a negative control [96].

Supplementary Information

The online version contains supplementary material available at <https://doi.org/10.1186/s12934-023-02036-y>.

Additional file 1: Figure S1. Neighbor-Joining (NJ) dendrograms showing the isolated *Trichoderma harzianum* based on 18S rRNA nucleotide sequences, respectively. Bootstrap values higher than 70 are shown below the branches of the trees.

Acknowledgements

The authors would like to thank the Academy of Scientific Research & Technology (ASRT) in Egypt for the fellowship awarded to Eman Abdallah.

Author contributions

Eman Abdallah and Mostafa Elshobary performed the experiments, the data analyses and wrote the manuscript; Refat Abdel-Basset contributed significantly to analysis and manuscript review; Mostafa Elshobary, Mostafa Elsheekh and Metwally Metwally reviewed the manuscript and performed the analysis with productive discussions. Mostafa Elshobary, Mostafa Elsheekh and Metwally Metwally contributed to the conception of the study. All authors have read and approved the final manuscript.

Funding

Open access funding provided by The Science, Technology & Innovation Funding Authority (STDF) in cooperation with The Egyptian Knowledge Bank (EKB).

Availability of data and materials

This article has all the data that was created or assessed during this study.

Declarations

Ethics approval and consent to participate

Not applicable.

Consent for publication

Not applicable.

Competing interests

The authors declare no competing interests.

Received: 14 January 2023 Accepted: 7 February 2023

Published online: 22 February 2023

References

- Babadi AA, Rahmati S, Fakhlaei R, Barati B, Wang S, Doherty W, Ostrikov K. Emerging technologies for biodiesel production: processes, challenges, and opportunities. *Biomass Bioenerg.* 2022;163:106521. <https://doi.org/10.1016/j.biombioe.2022.106521>.
- El-Seesy AI, Elshobary ME, He Z. Biofuel versus fossil fuel. In: El-Sheekh M, El-Fatah AA, editors. *Handbook of algal biofuels aspects of cultivation, conversion, and biorefinery.* Amsterdam: Elsevier; 2021. p. 181–93. <https://doi.org/10.1016/B978-0-12-823764-9.00027-3>.
- Abdelsalam I, Elshobary M, M. Eladawy M, Nagah M. Utilization of multi-tasking non-edible plants for phytoremediation and bioenergy source—a review. *Phyton (B Aires).* 2019;88:69–90. <https://doi.org/10.32604/phyton.2019.06831>.
- Abomohra AE, Elshobary M. Biodiesel, bioethanol, and biobutanol production from microalgae. *Microalgae biotechnol dev biofuel wastewater treat.* Singapore: Springer, Singapore; 2019. p. 293–321. https://doi.org/10.1007/978-981-13-2264-8_13.
- Shahbaz A, Hussain N, Saleem MZ, Saeed MU, Bilal M, Iqbal HMN. Nanoparticles as stimulants for efficient generation of biofuels and renewables. *Fuel.* 2022;319:123724. <https://doi.org/10.1016/j.fuel.2022.123724>.
- Sallam ER, Khairy HM, Elshobary M, Fetouh HA. Application of algae for hydrogen generation and utilization. In: El-Sheekh MM, Abdullah N, Ahmad I, editors. *Handbook of research on algae as a sustainable solution for food, energy, and the environment.* IGI Global: Hershey; 2022. p. 354–78. <https://doi.org/10.4018/978-1-6684-2438-4.ch014>.
- Prakasham RS, Sathish T, Brahmaiah P, Rao CS, Rao RS, Hobbs PJ. Biohydrogen production from renewable agri-waste blend: optimization using mixer design. *Int J Hydrogen Energy.* 2009;34:6143–8. <https://doi.org/10.1016/j.ijhydene.2009.06.016>.
- Liu H, Zhang Z, Lu C, Wang J, Wang K, Guo S, Zhang Q. Effects of enzymatic hydrolysis and alkalization pretreatment on biohydrogen production by *Chlorella* photosynthesis. *Bioresour Technol.* 2022;349:126859. <https://doi.org/10.1016/j.biortech.2022.126859>.
- Nayak BK, Roy S, Das D. Biohydrogen production from algal biomass (*Anabaena* sp. PCC 7120) cultivated in airlift photobioreactor. *Int J Hydrogen Energy.* 2014;39:7553–60. <https://doi.org/10.1016/j.ijhydene.2013.07.120>.
- Zayadan B, Kakimova A, Bolatkhan K, Sandybayeva S, Kosalbayev B, Nurabayeva D. Production of biohydrogen from cyanobacteria: current challenges and opportunities. *Int J Biol Chem.* 2021;14:4–20. <https://doi.org/10.26577/ijbch.2021.v14.i1.01>.
- Mahidhara G, Burrow H, Sasikala C, Ramana CV. Biological hydrogen production: molecular and electrolytic perspectives. *World J Microbiol Biotechnol.* 2019;35:1–13. <https://doi.org/10.1007/s11274-019-2692-z>.
- Yadav G, Sekar M, Kim SH, Geo VE, Bhatia SK, Sabir JSM, Chi NTL, Brindhadevi K, Pugazhendhi A. Lipid content, biomass density, fatty acid as selection markers for evaluating the suitability of four fast growing cyanobacterial strains for biodiesel production. *Bioresour Technol.* 2021;325:124654. <https://doi.org/10.1016/j.biortech.2020.124654>.
- Kossalbayev BD, Kakimova AB, Bolatkhan K, Zayadan BK, Sandybayeva SK, Bozieva AM, Sadvakasova AK, Alwasel S, Allakhverdiev SI. Biohydrogen production by novel cyanobacterial strains isolated from rice paddies in Kazakhstan. *Int J Hydrogen Energy.* 2022;47:16440–53. <https://doi.org/10.1016/j.ijhydene.2022.03.126>.
- Abdel-Kader HAA, Abdel-Basset R, Danial AW. Yeast and enzymatic hydrolysis in converting *Chlorella* biomass into hydrogen gas by *Rhodospirillum rubrum* sp. and *Rhodospirillum rubrum*. *Int J Hydrogen Energy.* 2022;47:1516–28. <https://doi.org/10.1016/j.ijhydene.2021.10.126>.
- Arhin SG, Cesaro A, Di Capua F, Esposito G. Recent progress and challenges in biotechnological valorization of lignocellulosic materials: towards sustainable biofuels and platform chemicals synthesis. *Sci Total Environ.* 2022;857:159333. <https://doi.org/10.1016/j.scitotenv.2022.159333>.
- Avargani VM, Zendejboudi S, Saady NMC, Dusseault MB. A comprehensive review on hydrogen production and utilization in North America: prospects and challenges. *Energy Convers Manag.* 2022;269:115927. <https://doi.org/10.1016/j.enconman.2022.115927>.
- Kumar SS, Himabindu V. Hydrogen production by PEM water electrolysis—a review. *Mater Sci Energy Technol.* 2019;2:442–54. <https://doi.org/10.1016/j.mset.2019.03.002>.
- Srivastava N, Hussain A, Kushwaha D, Haque S, Mishra PK, Gupta VK, Srivastava M. Nickel ferrite nanoparticles induced improved fungal cellulase production using residual algal biomass and subsequent hydrogen production following dark fermentation. *Fuel.* 2021;304:121391. <https://doi.org/10.1016/j.fuel.2021.121391>.
- Yang G, Wang J. Improving mechanisms of biohydrogen production from grass using zero-valent iron nanoparticles. *Bioresour Technol.* 2018;266:413–20. <https://doi.org/10.1016/j.biortech.2018.07.004>.
- Zhu X, He B, Zhao C, Fan R, Zhang L, Wang G, Ma Y, Yang W. Net-immobilization of β -glucosidase on nonwoven fabrics to lower the cost of "cellulosic ethanol" and increase cellulose conversions. *Sci Rep.* 2016;6:23437. <https://doi.org/10.1038/srep23437>.
- Du H, Deng F, Kommalapati RR, Amarasekara AS. Iron based catalysts in biomass processing. *Renew Sustain Energy Rev.* 2020;134:110292. <https://doi.org/10.1016/j.rser.2020.110292>.
- Pugazhendhi A, Shobana S, Nguyen DD, Banu JR, Sivagurunathan P, Chang SW, Ponnusamy VK, Kumar G. Application of nanotechnology (nanoparticles) in dark fermentative hydrogen production. *Int J Hydrogen Energy.* 2019;44:1431–40. <https://doi.org/10.1016/j.ijhydene.2018.11.114>.
- Rambabu K, Bharath G, Banat F, Hai A, Show PL, Nguyen THP. Ferric oxide/date seed activated carbon nanocomposites mediated dark fermentation of date fruit wastes for enriched biohydrogen production. *Int J Hydrogen Energy.* 2021;46:16631–43. <https://doi.org/10.1016/j.ijhydene.2020.06.108>.
- Rekha B, Saravanamurthy R. Catalytic conversion of corncob biomass into bioethanol. *Int J Energy Res.* 2021;45(3):4508–18. <https://doi.org/10.1002/er.6119>.
- Arantes MK, Sequinel R, Alves HJ, Machado B, Fiorini A, da Silva EA. Improvement of biohydrogen production from brewery wastewater: evaluation of inocula, support and reactor. *Int J Hydrogen Energy.* 2020;45:5216–26. <https://doi.org/10.1016/j.ijhydene.2019.07.208>.
- Harun I, Jahim JM, Anuar N, Hassan O. Hydrogen production performance by *Enterobacter cloacae* KBH3 isolated from termite guts. *Int J Hydrogen Energy.* 2012;37:15052–61. <https://doi.org/10.1016/j.ijhydene.2012.07.101>.
- Maintinguer SI, Lazaro CZ, Pachiega R, Varesche MBA, Sequinel R, de Oliveira JE. Hydrogen bioproduction with *Enterobacter* sp. isolated from brewery wastewater. *Int J Hydrogen Energy.* 2017;42:152–60. <https://doi.org/10.1016/j.ijhydene.2016.11.104>.
- El-Sheekh MM, Gheda SF, Ismail GA, Ghobashy RS. Green synthesis of silver nanoparticles from some cyanobacterial species. *Delta J Sci.* 2020;42:31–44.
- El Shafay SM, Gaber A, Alsanie WF, Elshobary ME. Influence of nutrient manipulation on growth and biochemical constituent in *Anabaena variabilis* and *Nostoc muscorum* to enhance biodiesel production. *Sustain.* 2021;13:9081. <https://doi.org/10.3390/su13169081>.
- Imai H, Chang K, Nakano S. Growth responses of harmful algal species *Microcystis* (Cyanophyceae) under various environmental conditions. *Interdiscip Stud Environ Chem Res Asia.* 2009; 269–275.
- Patel VK, Sundaram S, Patel AK, Kalra A. Characterization of seven species of cyanobacteria for high-quality biomass production. *Arab J Sci Eng.* 2018;43:109–21. <https://doi.org/10.1007/s13369-017-2666-0>.
- Hessami MJ, Phang SM, Salleh A, Rabiei R. Evaluation of tropical seaweeds as feedstock for bioethanol production. *Int J Environ Sci Technol.*

- Springer Berlin Heidelberg; 2018;15:977–92. <https://doi.org/10.1007/s13762-017-1455-3>.
33. Elshobary ME, El-Shenody RA, Abomohra AE, El-Shenody R, Abomohra AE. Sequential biofuel production from seaweeds enhances the energy recovery: a case study for biodiesel and bioethanol production. *Int J Energy Res.* 2020;45:1–11. <https://doi.org/10.1002/er.6181>.
 34. El-Sououd A, Ghada W, Morsy EM, Hassan LHS, El-Sheekh MM. Efficient Saccharification of the Microalgae *Chlorella vulgaris* and its Conversion into Ethanol by Fermentation. *Iran J Sci Technol Trans A Sci.* 2021;45(3):767–74. <https://doi.org/10.1007/s40995-021-01097-1>.
 35. Ashour M, Al-Souti AS, Hassan SM, Ammar GAG, Goda AMA-S, El-Shenody R, Abomohra AE-F, El-Haroun E, Elshobary ME. Commercial seaweed liquid extract as strawberry biostimulants and bioethanol production. *Life.* 2023;13:85. <https://doi.org/10.3390/life13010085>.
 36. Li K, Liu S, Liu X, Kexun L, Shun L, Xianhua L, Li K, Liu S, Liu X, Kexun L, Shun L, Xianhua L. An overview of algae bioethanol production. *Int J Energy Res.* 2014;38:965–77. <https://doi.org/10.1002/er.3164>.
 37. Ahmed S, Mustafa G, Arshad M, Rajoka MI. Fungal biomass protein production from *Trichoderma harzianum* using rice polishing. *Biomed Res Int.* 2017. <https://doi.org/10.1155/2017/6232793>.
 38. Singh H, Rout S, Das D. Dark fermentative biohydrogen production using pretreated *Scenedesmus obliquus* biomass under an integrated paradigm of biorefinery. *Int J Hydrogen Energy.* 2022;47(1):102–16. <https://doi.org/10.1016/j.ijhydene.2021.10.018>.
 39. Elsheekh M, Abdallah E, Abdelazeem M. Screening of cellulolytic activity of some Rhizospheric soil fungi isolated from different sources. *Delta J Sci.* 2022;44:88–100. <https://doi.org/10.21608/djs.2022.148953.1029>.
 40. da Silva DP, Farinas CS, da Silva Lima DJ, da Cruz Pradella JG. Experimental mixture design as a tool to enhance glycosyl hydrolases production by a new *Trichoderma harzianum* P49P11 strain cultivated under controlled bioreactor submerged fermentation. *Bioresour Technol.* 2013;132:401–5. <https://doi.org/10.1016/j.biortech.2012.11.087>.
 41. El-Shishtawy RM, Mohamed SA, Asiri AM, Gomaa AM, Ibrahim IH, Al-Talhi HA. Saccharification and hydrolytic enzyme production of alkali pre-treated wheat bran by *Trichoderma virens* under solid state fermentation. *BMC Biotechnol.* 2015;15:1–13. <https://doi.org/10.1186/s12896-015-0158-4>.
 42. Biswas P, Bharti AK, Kadam A, Dutt D. Wheat bran as substrate for enzyme production and its application in the bio-deinking of mixed office waste (MOW) paper. *Bioresour.* 2019;14:5788–806.
 43. Zhao Q, Lu D, Zhang G, Zhang D, Shi X. Recent improvements in enzyme-linked immunosorbent assays based on nanomaterials. *Talanta.* 2021;223:121722. <https://doi.org/10.1016/j.talanta.2020.121722>.
 44. de Pellegrini VOA, Sepulchro AGV, Polikarpov I. Enzymes for lignocellulosic biomass polysaccharide valorization and production of nanomaterials. *Curr Opin Green Sustain Chem.* 2020;26:100397. <https://doi.org/10.1016/j.cogsc.2020.100397>.
 45. Asar MF, Ahmad N, Husain Q. Chitosan modified Fe₃O₄/graphene oxide nanocomposite as a support for high yield and stable immobilization of cellulase: its application in the saccharification of microcrystalline cellulose. *Prep Biochem Biotechnol.* 2020;50(5):460–7. <https://doi.org/10.1080/10826068.2019.1706562>.
 46. Fokum E, Zabel HM, Ravikumary Y, Elshobary ME, Chandankere R, Zhang Y, Yun J, Qi X. Co-fermentation of glycerol and sugars by *Clostridium beijerinckii*: Enhancing the biosynthesis of 1,3-propanediol. *Food Biosci.* 2021;41:101028. <https://doi.org/10.1016/j.fbio.2021.101028>.
 47. Ngatcha AD, Muhammad G, Lv Y, Xiong W, Zhao A, Xu J, Alam MA. Microalgae biomass pre-treatment with deep eutectic solvent to optimize lipid isolation in biodiesel production. *Biomass Conv Bioref.* 2022; 12(S1):133–43. <https://doi.org/10.1007/s13399-021-02236-9>.
 48. Vishwakarma R, Malik A. Partial enzymatic cell wall disruption of *Oocystis* sp. for simultaneous cultivation and extraction. *Sep Purif Technol.* 2022;293:121107. <https://doi.org/10.1016/j.seppur.2022.121107>.
 49. Zanuso E, Ruiz HA, Domingues L, Teixeira JA. Magnetic nanoparticles as support for cellulase immobilization strategy for enzymatic hydrolysis using hydrothermally pretreated corn cob biomass. *BioEnergy Res.* 2022;15:1946–57. <https://doi.org/10.1007/s12155-021-10384-z>.
 50. Jiang J, Zhao J, He C, Cui B, Xiong J, Jiang H, Ao J, Xiang G. Recyclable magnetic carboxymethyl chitosan/calcium alginate – cellulase bioconjugates for corn stalk hydrolysis. *Carbohydr Polym.* 2017;166:358–64. <https://doi.org/10.1016/j.carbpol.2017.03.003>.
 51. Maffei G, Bracciale MP, Broggi A, Zuurro A, Santarelli ML, Lavecchia R. Effect of an enzymatic treatment with cellulase and mannanase on the structural properties of *Nannochloropsis* microalgae. *Bioresour Technol.* 2018;249:592–8. <https://doi.org/10.1016/j.biortech.2017.10.062>.
 52. Osorio LR, Meneguim AB, da Silva HB, Barreto HM, Osajima JA, da Silva Filho EC. Evaluation of physico-chemical properties and antimicrobial synergic effect of ceftazidime-modified chitosan. *J Therm Anal Calorim.* 2018;134(3):1629–36. <https://doi.org/10.1007/s10973-018-7332-6>.
 53. Zhang Y, Kang X, Zhen F, Wang Z, Kong X, Sun Y. Assessment of enzyme addition strategies on the enhancement of lipid yield from microalgae. *Biochem Eng J.* 2022;177:108198. <https://doi.org/10.1016/j.bej.2021.108198>.
 54. Dogan A, Siyakus G, Severcan F. FTIR spectroscopic characterization of irradiated hazelnut (*Corylus avellana* L.). *Food Chem.* 2007;100(3):1106–14. <https://doi.org/10.1016/j.foodchem.2005.11.017>.
 55. Ren L, Sun X, Zhang L, Huang H, Zhao Q. Exergy analysis for docosahexaenoic acid production by fermentation and strain improvement by adaptive laboratory evolution for *Schizochytrium* sp. *Bioresour Technol.* 2020;298:122562. <https://doi.org/10.1016/j.biortech.2019.122562>.
 56. Guido ES, Silveira JT, Kalil SJ. Enzymatic production of xylooligosaccharides from beechwood xylan: effect of xylanase preparation on carbohydrate profile of the hydrolysates. *Int Food Res J.* 2019;26(2):713–21.
 57. Zuurro A, Maffei G, Lavecchia R. Optimization of enzyme-assisted lipid extraction from *nannochloropsis* microalgae. *J Taiwan Inst Chem Eng.* 2016;67:106–14. <https://doi.org/10.1016/j.jtice.2016.08.016>.
 58. Zabel HM, Akter S, Yun J, Zhang G, Awad FN, Qi X, Sahu JN. Recent advances in biological pretreatment of microalgae and lignocellulosic biomass for biofuel production. *Renew Sustain Energy Rev.* 2019;105:105–28. <https://doi.org/10.1016/j.rser.2019.01.048>.
 59. Mustafa AH, Rashid SS, Rahim MHA, Roslan R, Musa WAM, Sikder BH, Sasi AA. Enzymatic pretreatment of lignocellulosic biomass: an overview. *J Chem Eng Ind Biotechnol.* 2022;8(1):1–7. <https://doi.org/10.15282/jceib.v8i1.7030>.
 60. Ramu SM, Thulasinathan B, Gajuluvu Hari D, Bora A, Jayabalan T, Mohammed SN, et al. Fermentative hydrogen production and bioelectricity generation from food based industrial waste: an integrative approach. *Bioresour Technol.* 2020;310:123447. <https://doi.org/10.1016/j.biortech.2020.123447>.
 61. Laxman Pachapur V, Jyoti Sarma S, Kaur Brar S, Le Bihan Y, Ricardo Soccol C, Buelna G, Verma M. Co-culture strategies for increased biohydrogen production. *Int J Energy Res.* 2015;39(11):1479–504. <https://doi.org/10.1002/er.3364>.
 62. Patel SKS, Kumar P, Mehariya S, Purohit HJ, Lee J-K, Kalia VC. Enhancement in hydrogen production by co-cultures of *Bacillus* and *Enterobacter*. *Int J Hydrogen Energy.* 2014;39:14663–8. <https://doi.org/10.1016/j.ijhydene.2014.07.084>.
 63. Kao P-M, Hsu B-M, Huang K-H, Tao C-W, Chang C-M, Ji W-T. Biohydrogen production by immobilized co-culture of *Clostridium butyricum* and *Rhodospirillum rubrum*. *Energy Procedia.* 2014;61:834–7. <https://doi.org/10.1016/j.egypro.2014.11.976>.
 64. Lackner M. Third-generation biofuels: bacteria and algae for better yield and sustainability. In: Lackner M, Sajjadi B, Chen WY, editors. *Handbook of climate change mitigation and adaptation*. Berlin: Springer; 2022. p. 1947–86. https://doi.org/10.1007/978-3-030-72579-2_90.
 65. Elsharnouby O, Hafez H, Nakhla G, El Naggat MH. A critical literature review on biohydrogen production by pure cultures. *Int J Hydrogen Energy.* 2013;38(12):4945–66. <https://doi.org/10.1016/j.ijhydene.2013.02.032>.
 66. Laurinavichene T, Laurinavichius K, Shastik E, Tsygankov A. Long-term H₂ photoproduction from starch by co-culture of *Clostridium butyricum* and *Rhodobacter sphaeroides* in a repeated batch process. *Biotechnol Lett.* 2018;40:309–14. <https://doi.org/10.1007/s10529-017-2486-z>.
 67. Zeidan AA, Rådström P, van Niel EWJ. Stable coexistence of two caldicellulosivor species in a de novo constructed hydrogen-producing co-culture. *Microb Cell Fact.* 2010;9:1–13. <https://doi.org/10.1186/1475-2859-9-102>.
 68. Ferraren-De Cagalitan DDT, Abundo MLS. A review of biohydrogen production technology for application towards hydrogen fuel cells. *Renew Sustain Energy Rev.* 2021;151:111413. <https://doi.org/10.1016/j.rser.2021.111413>.

69. Takagi H. Proline as a stress protectant in yeast: physiological functions, metabolic regulations, and biotechnological applications. *Appl Microbiol Biotechnol*. 2008;81(2):211–23. <https://doi.org/10.1007/s00253-008-1698-5>.
70. Elreedy A, Fujii M, Koyama M, Nakasaki K, Tawfik A. Enhanced fermentative hydrogen production from industrial wastewater using mixed culture bacteria incorporated with iron, nickel, and zinc-based nanoparticles. *Water Res*. 2019;151:349–61. <https://doi.org/10.1016/j.watres.2018.12.043>.
71. Srivastava N, Srivastava M, Malhotra BD, Gupta VK, Ramteke PW, Silva RN, Shukla P, Dubey KK, Mishra PK. Nanoengineered cellulosic biohydrogen production via dark fermentation: a novel approach. *Biotechnol Adv*. 2019;37:107384. <https://doi.org/10.1016/j.biotechadv.2019.04.006>.
72. Wang Y, Xiao G, Wang S, Su H. Application of nanomaterials in dark or light-assisted fermentation for enhanced biohydrogen production: a mini-review. *Bioresour Technol Rep*. 2023;21:101295. <https://doi.org/10.1016/j.biteb.2022.101295>.
73. Shanmugam S, Krishnaswamy S, Chandrababu R, Veerabagu U, Pugazhendhi A, Mathimani T. Optimal immobilization of *Trichoderma asperellum* laccase on polymer coated Fe₃O₄@SiO₂ nanoparticles for enhanced biohydrogen production from delignified lignocellulosic biomass. *Fuel*. 2020;273:117777. <https://doi.org/10.1016/j.fuel.2020.117777>.
74. Wiczorek N, Kucuker MA, Kuchta K. Fermentative hydrogen and methane production from microalgal biomass (*Chlorella vulgaris*) in a two-stage combined process. *Appl Energy*. 2014;132:108–17. <https://doi.org/10.1016/j.apenergy.2014.07.003>.
75. Wang J, Yin Y. Fermentative hydrogen production using pretreated microalgal biomass as feedstock. *Microb Cell Fact*. 2018;17:1–16. <https://doi.org/10.1186/s12934-018-0871-5>.
76. Henaish A. Physical and spectral studies of Mg-Zn ferrite prepared by different methods. *Arab J Nucl Sci Appl*. 2020;53(1):9–18. <https://doi.org/10.21608/ajnsa.2019.11102.1195>.
77. Prescott GW. How to know the freshwater algae. How to know Freshwater algae. Dubuque: Wm c. brown company publishers; 1964.
78. Guiry MD, Guiry G (2020) AlgaeBase. World-wide electronic publication, National university of Ireland, Galway. In: <http://www.algaebase.org/>
79. Rippka R, Deruelles J, Waterbury JB, Herdman M, Stanier RY. Generic assignments, strain histories and properties of pure cultures of cyanobacteria. *Microbiology*. 1979;111:1–61.
80. Lorenzen H. Synchronization of chlorella with light dark changes and periodical dilution to a standard cell number. New York: Inersci Pub; 1964. p. 571.
81. Elshobary ME, Osman MEH, Abushady AM, Piercey-Normore MD. Comparison of lichen-forming cyanobacterial and green algal photobionts with free-living algae. *Cryptogam Algal*. 2015;36:81–100. <https://doi.org/10.7872/crya.v36.iss1.2015.81>.
82. Huo S, Basheer S, Liu F, Elshobary M, Zhang C, Qian J, Xu L, Arslan M, Cui F, Zan X, Zhu F, Zou B, Ding Q, Ma H. Bacterial intervention on the growth, nutrient removal and lipid production of filamentous oleaginous microalgae *Tribonema* sp. *Algal Res*. 2020;52:102088. <https://doi.org/10.1016/j.algal.2020.102088>.
83. Tamura K, Stecher G, Kumar S. MEGA11: molecular evolutionary genetics analysis version 11. *Mol Biol Evol*. 2021;38:3022–7. <https://doi.org/10.1093/molbev/msab120>.
84. Saitou N, Nei M. The neighbor-joining method: a new method for reconstructing phylogenetic trees. *Mol Biol Evol*. 1987;4(4):406–25. <https://doi.org/10.1093/oxfordjournals.molbev.a040454>.
85. Felsenstein J. Confidence limits on phylogenies: an approach using the bootstrap. *Evolution* (N Y). 1985;39:783–91. <https://doi.org/10.2307/2408678>.
86. Wetherell DF. Culture of fresh water algae in enriched natural sea water. *Physiol Plant*. 1961;14:1–6. <https://doi.org/10.1111/j.1399-3054.1961.tb08131.x>.
87. Bradford MM. A rapid method for the quantitation of microgram quantities of protein utilizing the principle of protein-dye binding. *Anal Biochem*. 1976;72(7):248–54. <https://doi.org/10.1006/abio.1976.9999>.
88. Kochert G. Colony differentiation in green algae. In: Coward SJ, editor. Developmental regulation: aspects of cell differentiation. New York: Academic Press; 1973. p. 155–67.
89. Barakat KM, El-Sayed HS, Khairy HM, El-Sheikh MA, Al-Rashed SA, Arif IA, et al. Effects of ocean acidification on the growth and biochemical composition of a green alga (*Ulva fasciata*) and its associated microbiota. *Saudi J Biol Sci*. 2021;28(9):5106–14. <https://doi.org/10.1016/j.sjbs.2021.05.029>.
90. Hamouda RA, Hussein MH, El-Naggar NE-A. Potential value of red and brown seaweed for sustainable bioethanol production. *Bangladesh J Bot*. 2015;44(4):565–70. <https://doi.org/10.3329/bjb.v44i4.38571>.
91. Awais M, Fatma S, Naveed A, Batool U, Shehzad Q, Hameed A. Enhanced biodegradation of organic waste treated by environmental fungal isolates with higher cellulolytic potential. *Biomass Convers Biorefin*. 2021. <https://doi.org/10.1007/s13399-021-01932-w>.
92. Barman DN, Haque MA, Kang TH, Kim MK, Kim J, Kim H, Yun HD. Alkali pretreatment of wheat straw (*Triticum aestivum*) at boiling temperature for producing a bioethanol precursor. *Biosci Biotechnol Biochem*. 2012. <https://doi.org/10.1271/bbb.120480>.
93. Michalak I, Chojnacka K, Marycz K. Using ICP-OES and SEM-EDX in biosorption studies. *Microchim Acta*. 2011;172(1):65–74. <https://doi.org/10.1007/s00604-010-0468-0>.
94. Niu K, Zhang X, Tan W-S, Zhu M-L. Characteristics of fermentative hydrogen production with *Klebsiella pneumoniae* ECU-15 isolated from anaerobic sewage sludge. *Int J Hydrogen Energy*. 2010;35(1):71–80. <https://doi.org/10.1016/j.ijhydene.2009.10.071>.
95. Ludwig W, Schleifer K-H, Whitman WB. Revised road map to the phylum firmicutes. *Bergey's Man Syst Bacteriol*. 2009;2:1–8. <https://doi.org/10.1002/9781118960608.bm00025>.
96. El-Rab SMFG, Hifney AF, Abdel-Basset R. Costless and huge hydrogen yield by manipulation of iron concentrations in the new bacterial strain *Brevibacillus invocatus* SAR grown on algal biomass. *Int J Hydrogen Energy*. 2018;43(41):18896–907. <https://doi.org/10.1016/j.ijhydene.2018.08.116>.

Publisher's Note

Springer Nature remains neutral with regard to jurisdictional claims in published maps and institutional affiliations.

Ready to submit your research? Choose BMC and benefit from:

- fast, convenient online submission
- thorough peer review by experienced researchers in your field
- rapid publication on acceptance
- support for research data, including large and complex data types
- gold Open Access which fosters wider collaboration and increased citations
- maximum visibility for your research: over 100M website views per year

At BMC, research is always in progress.

Learn more biomedcentral.com/submissions

